https://doi.org/10.5194/egusphere-2026-4164
Preprint. Discussion started: 28 August 2026

The influence of snow on net ecosystem exchange over an alpine meadow in the Australian Alps.

Samuel H. Scott[1], Hamish A. McGowan[1]

[1]Weather and Climate Research Alliance, The University of Queensland, Brisbane 4072, Australia

Correspondence to: Samuel H. Scott (samuelhughscott2003@gmail.com)

Abstract.

Accurate modelling of climate change is underpinned by a robust understanding of the sources and sinks of carbon to the atmosphere. Currently, net ecosystem exchange over the distinct alpine meadow ecosystems of the Australian Alps has not been quantified, with limited understanding of the influence of environmental drivers such as snow, despite their sensitivity to climate change. We established an eddy covariance tower on an alpine meadow situated in the headwaters of the Pipers Creek catchment in the Australian Alps, collecting continuous half-hourly CO_2 fluxes from the 10^{th} June 2016 to the 19^{th} November 2019. The meadow functioned as a net carbon sink under snow-free conditions, transitioning to a net carbon source under snow-cover. This distinction was predominantly driven by the attenuation of photosynthetically active radiation and insulation of soil temperatures facilitated by the snowpack, preferentially inhibiting gross primary productivity. The site is found to be a stronger net carbon sink compared with other alpine meadow systems, globally, primarily due to a comparatively shorter snow-cover period. With the spatial and temporal extent of snowpacks in the Australian Alps anticipated to decrease under future climate scenarios, the sink strength of these alpine meadows is expected to increase.

1 Introduction

Net ecosystem exchange (NEE) over terrestrial ecosystems has been extensively researched amid escalating climate change concerns. However, the inherent heterogeneity of terrestrial landscapes coupled with the complex and multivariate influence of environmental drivers has left many ecosystems both under and unstudied, introducing uncertainty to global carbon modelling.

NEE is the net exchange of CO_2 between an ecosystem and the overlying atmosphere and represents the balance of ecosystem respiration (R_{eco}), driving CO_2 efflux, and gross primary production (GPP), driving CO_2 influx. The NEE dynamics of an ecosystem are governed by the prevailing weather and climate and biophysical properties (Hayek et al., 2018). Direct measurement of NEE is most accurately made using the eddy covariance (EC) technique, which measures the covariance between trace CO_2 concentrations and 3D wind velocity components. The EC technique has become the standard method for quantifying NEE over terrestrial ecosystems, presenting a non-invasive technique, capable of collecting continuous, in situ data over a prolonged period at the ecosystem level (Baldochii, 2003). This has ensured its widespread application, with over

https://doi.org/10.5194/egusphere-2026-4164
Preprint. Discussion started: 28 August 2026

1000 current and historic sites worldwide registered as part of the FLUXNET initiative to quantify land-atmosphere exchanges of carbon, energy, and moisture. Despite this global coverage, there are substantial knowledge gaps.

1.1 Net ecosystem exchange over alpine meadow communities

Globally, grasslands are one of the most widespread biomes, covering an estimated 22.8 % of the terrestrial landmass and storing an estimated 155.02 Gt of soil carbon (MacDougall et al., 2026). Within this biome, alpine meadows are characterised by a high soil carbon content and pronounced sensitivity to alterations in climate, driving concerns of future NEE dynamics and potential positive feedback loops (Knowles et al., 2019). Consequently, extensive research has been undertaken on these systems, though comparable studies on the Australian continent are rare.

Alpine meadows typically function as net carbon sinks, characterised by high incident solar radiation that enhances photosynthetic efficiency and low temperatures that constrain R_{eco} (Siato et al., 2009). This was demonstrated by Ma et al., (2023), who reported an annual NEE range between -308.75 ± 21.65 and 5.69 ± 18.24 g C m^2 yr^{-1} across eleven alpine meadow systems on the Qinghai-Tibet Plateau, with only one site functioning as a weak net carbon source. Similar results were reported by Marcolla et al. (2011) (Italian Alps), Koch et al. (2008) (Austria), and Sun et al. (2019) (Tibetan Plateau), though exhibiting varying sink strength. The distinct characteristics of individual systems, coupled with limited long-term records, hinder consensus on the NEE of alpine meadows. For instance, Knowles et al. (2019) (Colorado), Carrillo-Rojas et al. (2019) (Equatorian Andes), and Zhao et al. (2010) (Tibet) all reported alpine meadows as net carbon sources, some of which were associated with permafrost melt and the subsequent liberation of previously inaccessible carbon. Likewise, interannual variability complicates the determination of systems as net carbon sinks or sources (Marcolla et al., 2011). These unequivocal findings reiterate the necessity for site-specific quantifications of NEE over distinct ecosystems. This is especially the case for alpine meadows in the Australian Alps, where comparatively mild and short winters have created highly distinct systems.

Typically, NEE of alpine meadows exhibits seasonality, functioning as net carbon sinks under snow-free conditions and weak net carbon sources under snow-covered conditions (Zhao et al., 2010; Knowles et al., Koch et al., 2008). This is predominantly driven by seasonal variations in photosynthetically active radiation (PAR: 400-700 nm) and soil temperatures and their respective influences on GPP and R_{eco}, which is largely modulated by snow cover. However, there is substantial spatiotemporal variation in the dominant drivers, with leaf area index and soil water content remaining key predictors, both of which are influenced by snow cover (Saito et al., 2009; Koch et al., 2008; Wang et al., 2025).

1.2 Influence of snow on gross primary productivity

Gross primary productivity represents the carbon uptake driven by autotrophic photosynthesis. In photosynthesis, the photochemical component is governed by the availability of solar radiation, whereas the biochemical component is governed by concentrations of CO_2, temperature, as well as the supply of water and mineral nutrients (Saito et al., 2009; Schulze and Caldwell, 1995). Under snow-covered conditions, low temperatures and reduced PAR substantially dampen photosynthetic activity. Temperatures below zero lower the efficiency of biochemical processes, with vascular plants typically operating at

20-30 % of their maximum capacity at 0°C, decreasing further with subsequent temperature drops (Körner, 2021). These rates are further dampened by the reduced availability of PAR under snow-covered conditions, an effect that becomes more substantial as snow depth increases, constraining photochemical processes.

Snowpacks attenuate PAR by reflection at the surface (albedo) and extinction through the snowpack (Körner, 2021; Robson and Aphalo, 2019). Characterised by high surface albedo, snowpacks reflect between 60 and 90% of incident shortwave radiation. The reflectiveness of snowpacks is governed by characteristics including grain size, shape, liquid water content, surface roughness, and presence of impurities, as well as prevailing environmental factors including solar zenith angle, cloud conditions, and the underlying surface characteristics of thin snowpacks (Zhang, 2005).
The minimal irradiance absorbed by the snowpack diminishes precipitously with depth through backscattering and absorption processes (Robson and Aphalo, 2019), with an estimated <10 % of incident PAR penetrating to a depth of 10 cm, reducing to 2-3 % at 20 cm and negligible at a depth greater than 30cm (Körner, 2003; Robson and Aphalo, 2019). Additionally, snowpacks disrupt the incident spectral composition of PAR by preferentially adsorbing longer wavelengths, associated with red light, over shorter wavelengths, associated with blue and green light. This further inhibits photochemical processes, as red light wavelengths are most efficiently utilised during photosynthesis, particularly under low light conditions (McCree, 1972; Liu and van Lersel, 2021).

1.3 Influence of snow on ecosystem respiration

Ecosystem respiration is the combined sum of autotrophic and heterotrophic respiration in an ecosystem and is dominated by soil respiration (Knowles et al., 2015). Consequently, R_{eco} is largely determined by soil temperature, which governs the metabolic rate of soil microbes (Skinner, 2007; Saito et al., 2009; Warren and Taranto, 2011). Snow has a low thermal conductivity that insulates the underlying ground. In doing so, it reduces diurnal fluctuations in soil temperature, maintaining a threshold that facilitates both plant and soil respiration (Körner, 2021; Warren and Taranto, 2011; Merbold, Rogiers and Eugster, 2012; Zhang, 2005). Similarly, it lowers the frequency and depth of soil freezing events, preventing associated drops in soil microbial biomass, diversity, and activity (Warren and Taranto, 2011; Sorensen et al., 2018). This enables R_{eco} to continue under snow-covered conditions, often transitioning ecosystems to net carbon sources, with the snow preferentially inhibiting GPP (Hubbard et al., 2005; Monson et al., 2006; Reverter et al., 2010; Pullen et al., 2016; Euskirchen et al., 2012).

The insulating potential of snowpacks is proportionate to depth (Merbold, Rogiers, and Eugster, 2012; Zhang, 2005). As snow depth increases, soil temperatures and R_{eco} stabilise, typically plateauing at a snow depth of 40 to 60 cm, at which depth the insulating potential of the snowpack is maximised (Smith, 1975; Merbold, Rogiers, and Eugster, 2012; Zhang, 2005). To this end, thinner snowpacks typically exhibit lower R_{eco}, reflecting the diminished insulation potential of the overlying snowpack (Monson et al., 2006). The snowpacks of the Australian Alps are characterised as marginal and shallow relative to those situated in higher latitudes and altitudes, where most research has been undertaken on the influence of snow on NEE (Warren

https://doi.org/10.5194/egusphere-2026-4164
Preprint. Discussion started: 28 August 2026

and Taranto, 2010). The Australian snowpacks likely permit lower rates of R_{eco} under snow-covered conditions relative to those cited in the current literature (Sect. 1.3). Likewise, shallow snowpacks attenuate less PAR, facilitating higher rates of GPP. Thus, it is also probable that the marginal snowpacks of the Australian Alps permit higher rates of GPP under snow-covered conditions, with alpine meadows potentially functioning as net carbon sinks year-round.

Here we present the first observations of NEE over an alpine meadow ecosystem in the Australian Alps using the EC method. We analyse the individual and combined influences of meteorological variables on NEE, GPP and R_{eco}, over diurnal and seasonal timescales, under snow-free and snow-covered conditions, to evaluate the influence of snow on CO_2 fluxes in the Australian Alps.

2 Physical setting

2.1 Regional context

The Australian Alps span approximately 1.6 million hectares in the southern extent of the Great Dividing Range and include the tallest peak on the Australian continent, Mt. Kosciuszko (2228 m a.s.l.) (Department of Climate Change, Energy, the Environment and Water, 2023). The prevailing temperate climate is characterised by cool to mild summers with no distinct dry season and a cold and wet winter season (Stern, de Hoedt, and Ernst, 2000; Sahukar et al., 2003). The region is unique in Australia, being the only mainland area that regularly receives rainfall year-round (Gunawardhana et al., 2025). Precipitation primarily falls as snow between June and September, coinciding with the northward movement of the subtropical ridge, enabling cold fronts to pass over the region (Chubb et al., 2011; Theobold et al., 2016; Schwartz et al., 2021). This precipitation ensures a valuable ecosystem service, accounting for 29 % of the inflow yield into the 1.06 km^2 Murray-Darling Basin. This generates economic activity estimated at around $9.6 billion annually, facilitating downstream agricultural and industrial activities, and simultaneously producing hydroelectric power (Worboys and Good, 2011).

In the Australian Alps, snowpacks exhibit substantial intra- and inter-annual variability, typically forming in late May to June, before ablating in mid-September to October (Bilish et al., 2019; Snowy Hydro Ltd, 2023). The snowpack is classified as marginal with the relatively mild air and soil temperatures combining with high incident solar radiation to create a dense, isothermal snowpack that exhibits basal melt and relatively constant ablation (Bilish et al., 2018; Bilish et al., 2019; Schwartz et al., 2020a; Schwartz et al., 2020b).

The region is within the Australian Alps bioregion (Sahukar et al., 2003), with the majority classified as sub-alpine, and only 250 km^2 considered truly alpine, 100 km^2 of which is centred on Mt Kosciuszko above approximately 1830 m (Costin et al., 2000).

https://doi.org/10.5194/egusphere-2026-4164
Preprint. Discussion started: 28 August 2026

2.2 Study site

The study site is located in the headwaters of the Pipers Creek catchment within the Australian Alps (36.418° S, 148.422° E, 1847 m a.s.l; Fig. 1e) (Schwartz, 2021) and within an ecotone between alpine and sub-alpine zones, featuring vegetation communities characteristic of both (Ecology Australia Pty Ltd, 2003; Sahukar et al., 2003). These vegetation communities have been described as upper sub-alpine (*Eucalytpus pauciflora*) woodland, tall alpine heathlands, sod tussock grassland, upland and valley bogs (Ecology Australia Pty Ltd, 2003; Connell Wagner Pty Ltd, 2000) with sod tussock grassland representative of the target alpine meadow ecosystem. Grassland species associated with the study site include *Poa hiemata*, *Poa costiniana*, *Rytidosperma nudiflorumi* (Ecology Australia Pty Ltd).

To provide context on the prevailing bioclimatic properties of the study site, climate data was obtained from the Australian Bureau of Meteorology Perisher Valley AWS weather station #071075, located approximately 1.25 km northwest of the study site (36.41° S, 148.41° E, 1738 m a.s.l) . The site receives 2138.16 mm precipitation annually, exhibiting substantial interannual variability, recording a range of 1300 mm between 2010 and 2025 (Bureau of Meteorology, 2026). Maximum and minimum temperatures during summer are 18.26°C and 6.24°C, and 3.70°C and -3.46°C during winter, respectively.

https://doi.org/10.5194/egusphere-2026-4164
Preprint. Discussion started: 28 August 2026

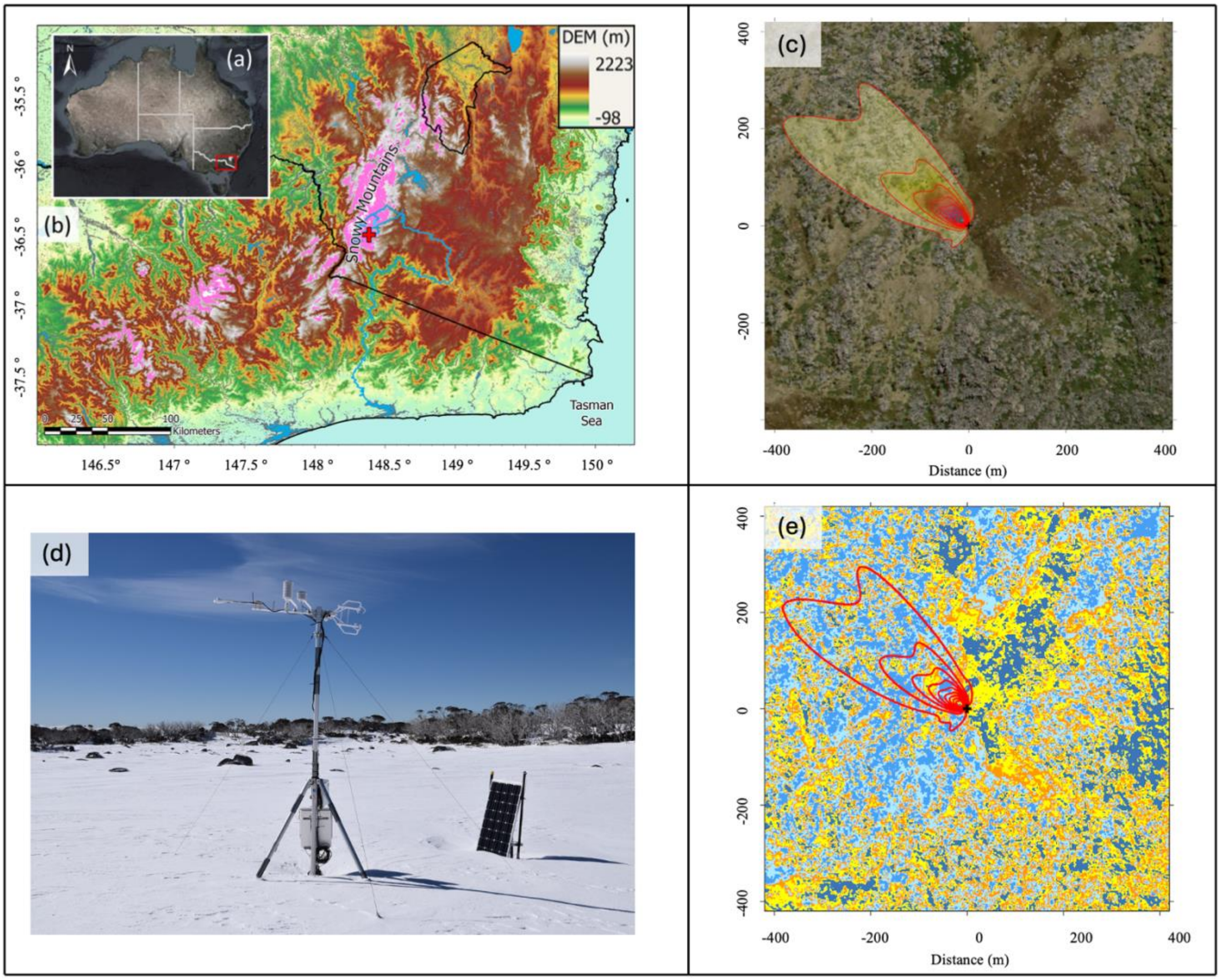

Fig. 1. Study area: (a) location of study region within Australian continent, (b) location of study site within regional digital elevation model (DEM) of the Australian Alps (site indicated by '+'), (c) two-dimensional flux footprint prediction (FFP) model output from 10 June 2025 to 31 December 2017 (red contours denote 10 % isopleths; base image © 2025 google), (d) eddy covariance instrumentation set up at study site under snow-covered conditions (26 July 2018), (e) FFP overlaid with unsupervised land classification map, derived from red-green-blue spectrum analysis of google satellite imagery.

3.0 Methods

3.1 Data collection

Direct measurement of CO_2 fluxes was undertaken from the 10th June 2016 to the 19th November 2019 using an EC tower (Figure 1e). The EC system comprised a Campbell Scientific CSAT3 sonic anemometer paired with an EC150 infrared open-path gas analyser mounted at a height of 3 m above the ground surface, sampling at 10 Hz. Ambient air temperature and

https://doi.org/10.5194/egusphere-2026-4164
Preprint. Discussion started: 28 August 2026

relative humidity were measured using a Vaisala HMP155 probe installed at approximately 3.1 m. Incoming and outgoing shortwave radiation were measured using a Kipp and Zonen CNR4 radiometer installed at 3 m. Soil temperature was measured using a Campbell Scientific CS650 installed at a depth of 5 cm. PAR, snow depth, and barometric pressure were measured using a LICOR LI-190SB Quantum sensor, a Sommer USH-8 ultrasonic snow depth sensor, and a Vaisala PTB110 sensor, respectively. CO_2 fluxes and accompanying meteorological data were aggregated into 30-minute average blocks using a Campbell Scientific CR3000 micrologger running the EasyFlux DL software. Instrument specifications are presented in Table 1.

Table 1. Study site instrumentation.

Instrument and manufacturer	Manufacturer	Variables measured	Accuracy/resolution
CSAT3A	Campbell Scientific (USA)	3-D wind components, wind speed and direction, and sonic temperature	± 5 cm s^{-1}
EC150	Campbell Scientific (USA)	CO_2 gas density	2 %
HMP155	Vaisala (Finland)	Air temperature, relative humidity	< 0.3 ℃ <1.8 % RH
CNR4	Kipp and Zonen (The Netherlands)	Incoming and outgoing shortwave radiation	< 5 % Daily Total
CS650	Campbell Scientific (USA)	Soil water content, soil temperature	± 3 % SWC ± 5℃
LI-190SB	LICOR (USA)	Photosynthetically active radiation (PAR)	< 1%
USH-8	Sommer (Austria) (Austria)	Snow depth	0.1 % of range 0 – 8 m
PTB110	Vaisala (Findland)	Barometric pressure	± 0.15 kPa

3.2 Flux footprint prediction model

To ensure CO_2 flux data was representative of the target ecosystem, a flux footprint prediction model (FFP), adapted from Kljun et al. (2015), was developed to determine the spatial origins of CO_2 fluxes. The resulting FFP showed most fluxes originated northwest of the EC tower, with the 90^{th} percentile extending approximately 400 m. When overlayed with an unsupervised land classification (Figure 1e) and surface vegetation map, the FFP primarily captured the target sod-tussock

https://doi.org/10.5194/egusphere-2026-4164
Preprint. Discussion started: 28 August 2026

grassland community, with some marginal upper sub-alpine (*Eucalyptus pauciflora*) woodland and tall alpine heathlands communities featuring within the 80th to 90th isopleths. Fluxes within these isopleths have not been excluded from the final flux dataset, due to the marginal nature of non-target ecosystem patches and their subsequent marginal influence on the overall NEE.

3.3 Data processing and corrections

The raw 10 Hz EC data were corrected using a double rotation method adapted from Stiperski and Rotach (2016) to correct for potential errors caused by imprecise instrument levelling, as well as to remove larger-scale signals associated with thermally driven anabatic and katabatic flows. Fluxes were corrected for both sensor response delays and the spatial separation between the sonic anemometer and gas analyser. Air density corrections adapted from Webb et al. (1980) were applied to consider vertical velocities derived from changes in water vapor and heat content. Flux data was despiked following a three-step process. First, implausible values were removed upon visual inspection. Second, flux records associated with a water vapour signal strength of < 0.7 were removed to minimise errors associated with precipitation on the sensor lenses (Gray et al., 2018), and finally, a 6-point moving average filter was applied to the flux dataset over three iterations, removing values exceeding three standard deviations from the average moving window (Vickers and Mahrt, 1997). Data gaps less than 90 minutes were filled using linear interpolation (Falge et al., 2001a, Falge et al., 2001b).

3.4 Data post-processing

To alleviate bias associated with underestimation of nighttime fluxes, fluxes recorded during periods of low turbulence were removed with a site- and season-specific u* threshold that was applied using a moving point method adapted from Papale et al. (2006). The u* filtering excluded 37 % of half-hourly flux observations, requiring 59.5 % of the original dataset to be gap-filled following the previous data processing and correction methods. Gap-filling was undertaken using a marginal distribution sampling (MDS) method adapted from Reichstein et al. (2005a). This method first integrated a look-up table method, identifying fluxes recorded under similar meteorological conditions - specifically incident shortwave radiation, ambient air temperature, and vapour pressure deficit - within a defined moving time window of seven days. During periods of insufficient meteorological data, a mean diurnal cycle (MDC) method was adopted, averaging fluxes recorded at the same time of day in the adjacent time windows.

A persistent data gap from 27 March 2018 to 20 June 2018 due to instrument failure remained too large to accurately fill and, therefore, remains unfilled in the resulting dataset, which contains 56,257 half-hourly measurements of CO_2 flux. The resulting quality-controlled, gap-filled half-hourly NEE dataset was partitioned into its primary components - GPP and R_{eco} - using the standardized methods established in Reichstein et al. (2005b, c). This approach modelled nighttime NEE, which is equivalent to R_{eco} in the absence of photosynthetic activity, as a function of temperature in accordance with the Lloyd and Taylor (1994), model. This association was then extrapolated to daytime conditions to estimate daytime R_{eco}. GPP values were calculated as the difference between modelled R_{eco} and observed NEE. The REddy Proc R-package (version 1.3.3, Wultzer et al., 2024) was

https://doi.org/10.5194/egusphere-2026-4164
Preprint. Discussion started: 28 August 2026

utilised for u* filtering, gap filling, and flux partitioning post-processing steps (Wultzer et al., 2018), and was selected due to its application in comparable studies (Carrillo-Rojas et al., 2019; Michael and Seneviratne, 2022).

3.5 Summary statistics and analysis

To investigate the influence of prevailing meteorological conditions on CO_2 fluxes during snow-free and snow-covered conditions, a series of statistical analyses was undertaken. Firstly, the Pearson correlation method was used to establish linear associations between individual meteorological variables and CO_2 fluxes. Secondly, a random forest machine learning algorithm (RF) was used to determine the combined influence of meteorological variables on CO_2 fluxes using the “randomForest” R-package (version 4.7-1.2, Liaw and Wiener, 2002; Brieman, 2001). The RF variable importance scores for meteorological variables – indicating the relative importance of predictors in determining response variables were calculated as the percent increase in mean squared error resulting from random permutation of each meteorological variable.
Thirdly, a generalised additive model (GAM) was developed to model the combined influence of meteorological variables on NEE during snow-free and snow-covered conditions using the ‘mgcv’ R-package (version 1.9-4; Wood, 2011).
A GAM explains the non-linear relationship between a series of predictors and a single response variable by modelling the response variable as an additive sum of a smooth function in accordance with Eq. (1).

$$Y = c + f_1(x_1) + f_2(x_2) \ldots + f_n(x_n) + \varepsilon \ , \qquad (1)$$

where Y is the response variable, x is the predictor, f is the smooth function, c is the baseline value, and ε is the error term. Thin-plate splines are then utilised to construct smooth functions of each explanatory variable (Hastie and Tibshirani, 1986; Wood, 2017). The fitness and smoothness of these smooth functions are optimised using a smoothing parameter selected by the restricted marginal likelihood (REML) method. This is a form of maximum likelihood estimation that derives a likelihood function from a transformed dataset to render nuisance parameters redundant (Pal and Chakravarty, 2020).

Meteorological variables were selected for the GAM with consideration of RF variable importance scores and concurvity, where the influence of one explanatory variable can be explained by another, introducing model redundancy.

Snow-covered conditions were defined by a snow depth greater than 30 cm, based on the mean height of grassland vegetation at the study site. As snow depth was not recorded during 2016, the winter months of 2016 were excluded from the subset datasets. Snow-free and snow-covered datasets were established between the 19th of November 2016 and the 19th of November 2019, providing three complete years of CO_2 flux and snow-depth data, excluding a data gap from 27 March 2018 to 20 June 2018. Snow-free and snow-covered datasets included 864 and 232 days, respectively.

To establish ecosystem CO_2 flux characteristics at varying temporal scales, both diurnal and seasonal trends were analysed. Diurnal trends were analysed using mean half-hourly CO_2 fluxes (μmol CO_2 m^{-2} s^{-1}) and corresponding meteorological variables, whilst seasonal trends were analysed using daily CO_2 fluxes (g C m^{-2} day^{-1}) and daily averaged meteorological variables. Precipitation data, obtained from the Perisher Valley AWS weather station #071075, were confined to daily totals

https://doi.org/10.5194/egusphere-2026-4164
Preprint. Discussion started: 28 August 2026

and therefore have only been used for seasonal analysis. Negative NEE values correspond to net carbon influx whilst positive NEE values correspond to net carbon efflux.

4.0 Results

4.1 Prevailing meteorological conditions

The prevailing meteorological conditions of ambient air temperature (Tair), soil temperature (Tsoil), PAR, vapour pressure deficit (VPD), wind speed (WS), relative humidity (RH), precipitation (PPT), and snow depth (SD) during the measurement period from the 10th June 2016 to the 19th November 2019 are presented in Fig. 2. Air temperature (Tair), soil temperature (Tsoil), PAR, and to a lesser extent vapour pressure deficit (VPD), all exhibited a similar seasonal trend of peaking during summer before subsiding during winter. Tsoil plateaued around 0 °C during winter, coinciding with the formation of the snowpack. Conversely, wind speed (WS) peaks during winter, reflecting the seasonal impact of cold fronts on the Australian Alps. Relative humidity (RH) and precipitation (PPT) exhibited no seasonal trend, with both remaining random throughout the study period.

The snow depth (SD) exhibited substantial interannual variability in both duration and maximum depth. In 2017, the snowpack began to form in July, reaching a maximum depth of 120 cm and prevailing for 68 days. In 2018, the snowpack commenced in June, reaching a maximum depth of only 76 cm, but prevailing for 20 days longer at 88 days. In 2019, the snowpack began to accumulate in May, reaching a maximum depth of 105 cm and prevailing for 90 days. The study site returned to snow-free conditions in late September for all years.

https://doi.org/10.5194/egusphere-2026-4164
Preprint. Discussion started: 28 August 2026

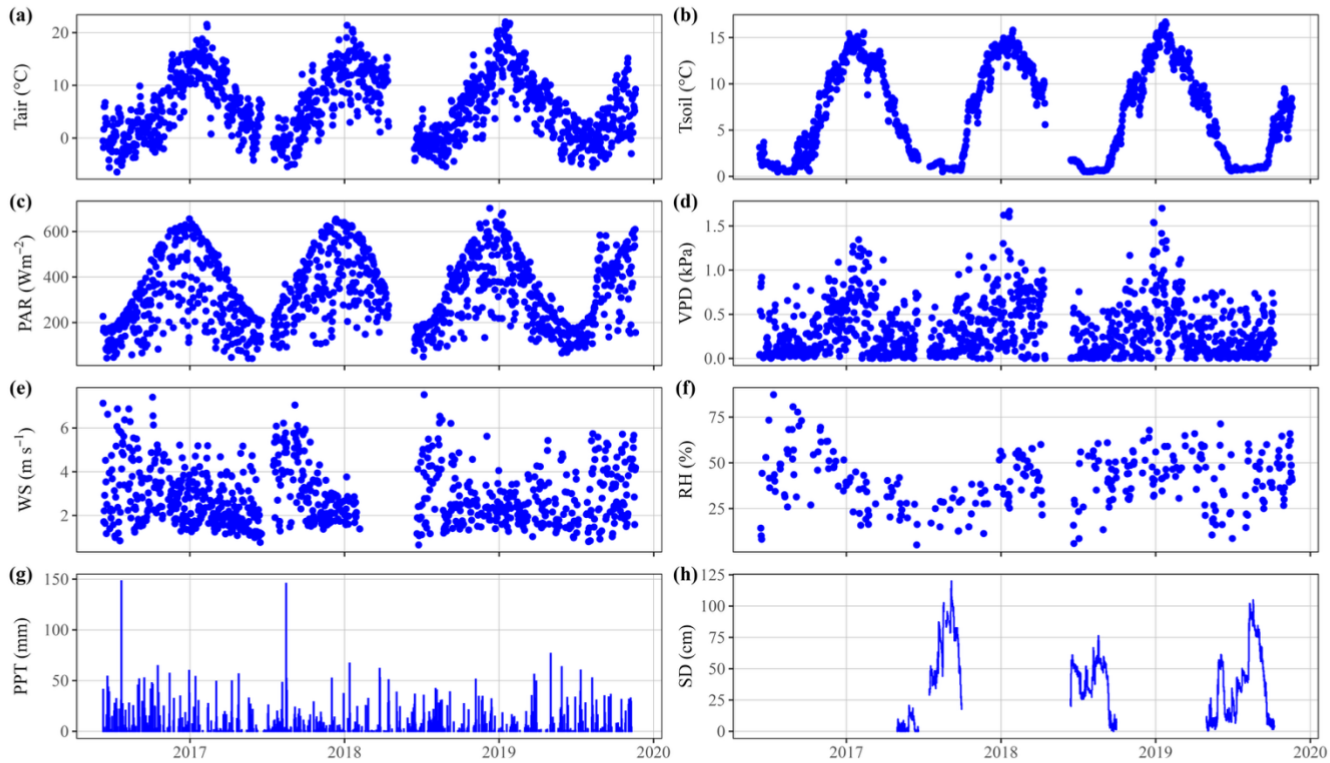

Fig. 2. Prevailing meteorological conditions: (a) daily average ambient air temperature (Tair), (b) daily average soil temperature (Tsoil), (c) daily average photosynthetically active radiation (PAR), (d) daily average vapour pressure deficit (VPD), (e) daily average wind speed (WS), (f) daily average relative humidity (RH), (g) daily total precipitation (PPT), (h) daily average snow-depth (SD)

4.2 Seasonal variations in CO_2 fluxes

A half-hourly fingerprint plot of NEE fluxes is presented in Fig. 3a, alongside daily and cumulative values of NEE, GPP, and R_{eco} in Fig. 3b and 3c, respectively. In line with prevailing conditions of Tair, Tsoil, and PAR, CO_2 fluxes exhibited clear seasonality throughout the study period. Under snow-free conditions, NEE remained consistently negative, with a mean daily influx of -1.13 g C m^{-2} day^{-1}. This was driven by higher GPP compared to R_{eco}, with mean daily flux of 4.43 g C m^{-2} day^{-1} and 3.21 g C m^{-2} day^{-1}, respectively. Conversely, under snow-covered conditions, NEE remained consistently positive, with a mean daily efflux of 1.44 g C m^{-2} day^{-1}. Similarly, this was driven by lower GPP compared to R_{eco}, with mean daily flux of 0.50 g C m^{-2} day^{-1} and 1.95 g C m^{-2} day^{-1}, respectively. GPP exhibited greater seasonality with a seasonal flux range of 12.21 g C m^{-2} day^{-1} relative to 8.13 g C m^{-2} day^{-1} for R_{eco}.

Accordingly, the site functioned as a net carbon sink under snow-free conditions, transitioning to a net carbon source under snow-covered conditions. This mirrored cumulative plots of NEE, with negative inclines of carbon influx corresponding with snow-free conditions and positive inclines of carbon efflux corresponding with snow-covered conditions, driven by differential gradients in GPP and R_{eco}.

https://doi.org/10.5194/egusphere-2026-4164
Preprint. Discussion started: 28 August 2026

Interannually, the study site exhibited substantial variability. The site functioned as a net carbon sink for all complete survey years (July to June), though varying in sink strength. In 2016/17, cumulative NEE was -246.64 g C m^2 yr^{-1}, with the site functioning as a net carbon sink for 61 % of the year. In 2017/18, cumulative NEE rose to -309.99 g C m^2 yr^{-1} and functioned as a net carbon sink for 59 % of the year, though a data gap between 27 March 2018 and 20 June 2018 skewed summary statistics to reflect a stronger relative carbon sink. In 2018/19, cumulative NEE dropped to a low of -93.98 g C m^2 yr^{-1} and functioned as a net carbon sink for 56 % of the year.

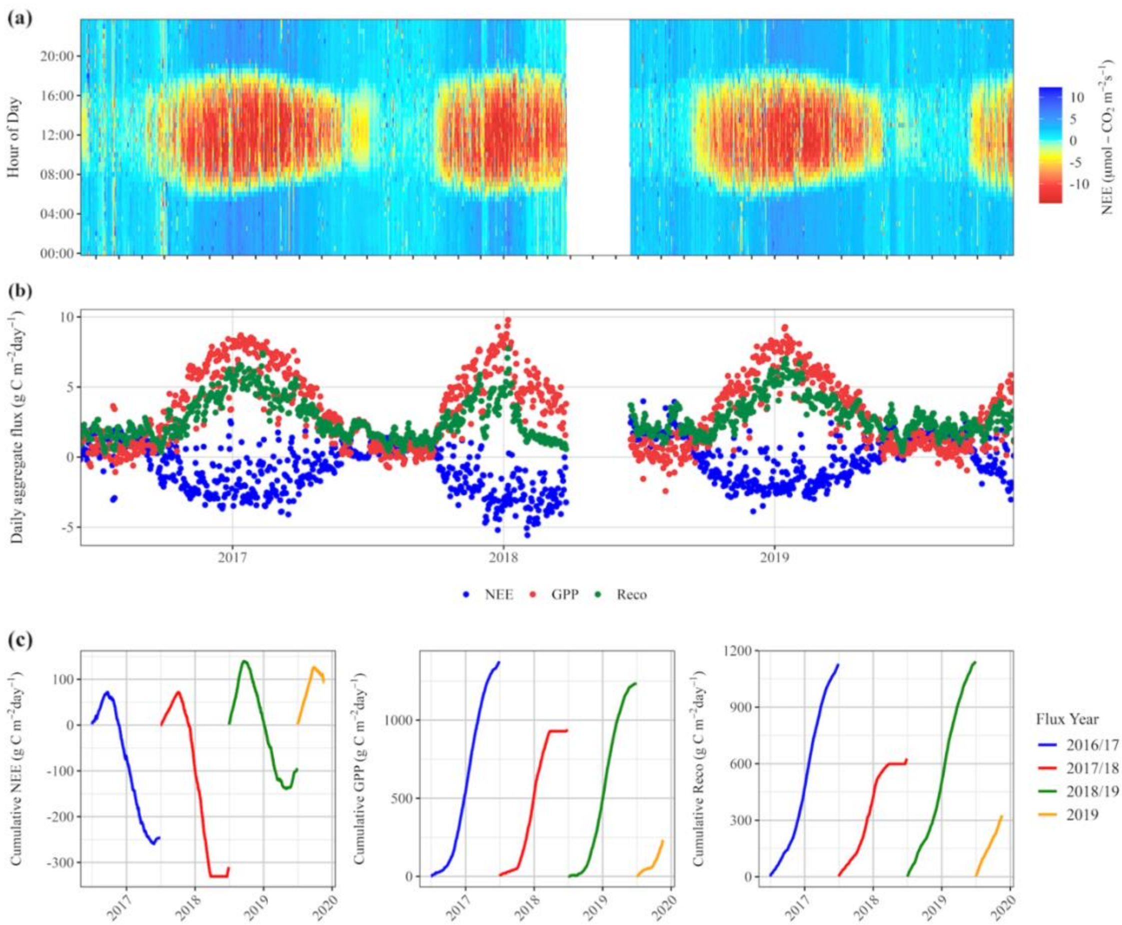

Fig. 3. (a) half-hourly NEE fingerprint, (b) daily fluxes of CO_2 fluxes, (c) annual cumulative CO_2 fluxes, from 01-July to 31-June. Positive slopes denote carbon efflux and negative slopes denote carbon influx.

4.3 Diurnal variations of CO_2 fluxes

Diurnal plots of NEE, GPP, and R_{eco} during snow-free and snow-covered conditions are presented in Fig. 4a, 4b, and 4c, respectively. Under snow-free conditions, NEE exhibited a pronounced diurnal trend. During nighttime hours from 19:30 AEST to 05:00 AEST, NEE was stable and positive, plateauing at approximately 2.78 µmol CO_2 m^{-2} s^{-1}. This is reminiscent

https://doi.org/10.5194/egusphere-2026-4164
Preprint. Discussion started: 28 August 2026

of NEE being equivalent to R_{eco} in the absence of PAR and subsequent photosynthetic activity. During daylight hours from 05:30 AEST to 19:00 AEST, NEE exhibited a pronounced U-shaped trend, becoming negative between 07:00 AEST and 17:30 AEST and reaching a minimum of -7.67 µmol CO_2 m^{-2} s^{-1} at 11:30 AEST. This is reflective of GPP becoming the dominant influence on NEE, as photosynthetic activity resumes with the influx of PAR. Ultimately, daytime NEE influx exceeded nighttime NEE efflux, rendering the site a net carbon sink under snow-free conditions.

Under snow-covered conditions, diurnal trends in NEE were substantially dampened, with a diel range of 1.61 µmol CO_2 m^{-2} s^{-1} relative to 10.52 µmol CO_2 m^{-2} s^{-1}, under snow-free conditions. During nighttime hours from 18:00 AEST to 07:00 AEST, NEE was stable and positive, plateauing at 1.85 µmol CO_2 m^{-2} s^{-1}. Akin to snow-free conditions, this is indicative of NEE being equivalent to R_{eco}, with nighttime R_{eco} remaining slightly lower under snow-covered conditions. During daytime hours from 07:30 AEST to 17:30 AEST, NEE exhibited a slight U-shaped trend, reaching a minimum of 0.41 µmol CO_2 m^{-2} s^{-1} around midday. Under snow-covered conditions, NEE remained positive, rendering the site a net carbon source.

Whilst both GPP and R_{eco} were constrained under snow-covered conditions, GPP was disproportionately inhibited. Additionally, GPP was the dominant component of NEE, indicated by the close mirroring in diurnal trends between NEE and GPP.

https://doi.org/10.5194/egusphere-2026-4164
Preprint. Discussion started: 28 August 2026

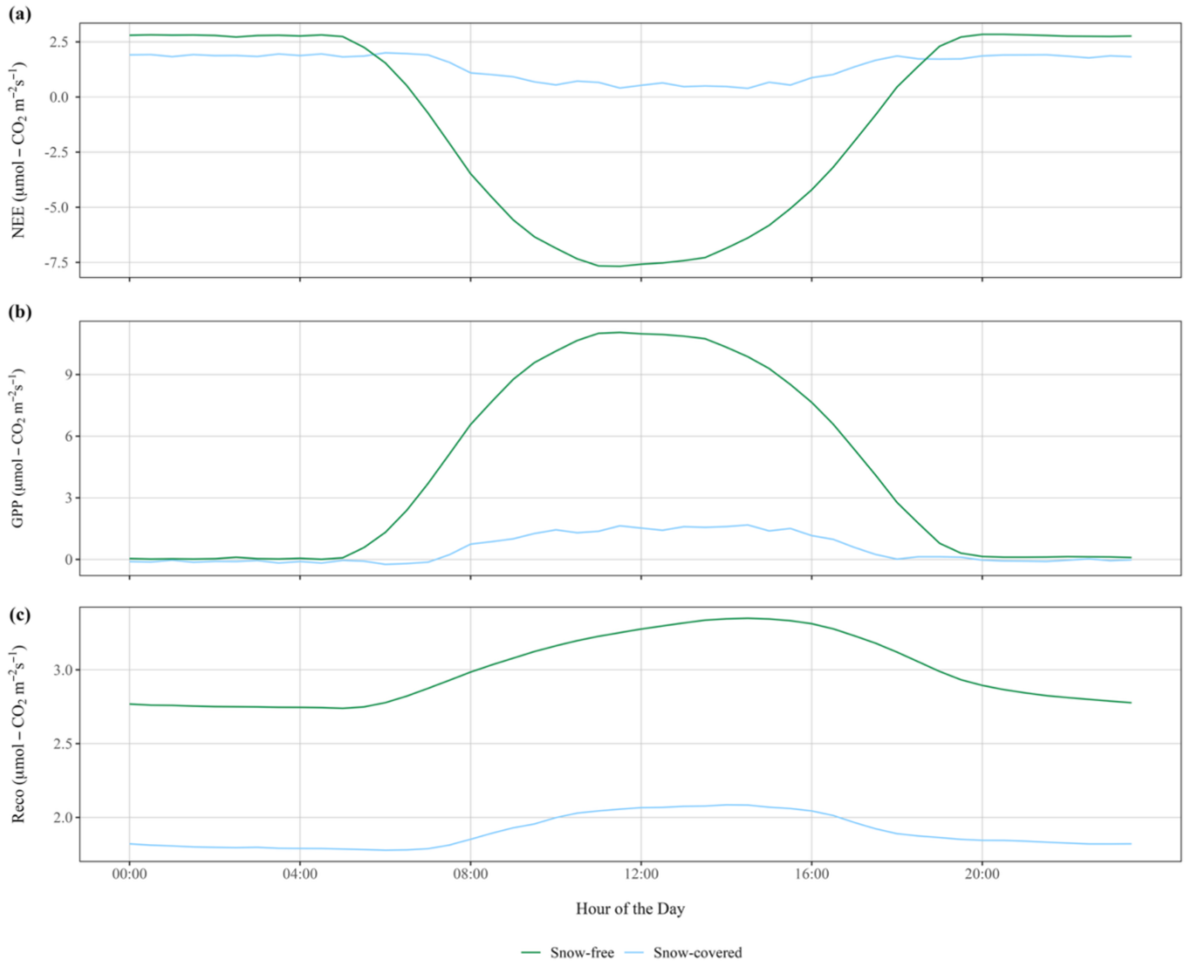

Fig. 4. Diurnal CO_2 fluxes under snow-free and snow-covered conditions, (a) NEE (b) GPP (c) R_{eco}.

4.4 Meteorological influences on CO_2 fluxes

A Pearson correlation matrix between meteorological predictors and CO_2 fluxes under snow-free and snow-covered conditions at half-hourly and daily timescales is presented in Fig. 5. Under snow-free conditions, half-hourly NEE exhibited a strong negative linear association with PAR, which mirrored a comparatively strong positive linear association between GPP and PAR. This close association largely explains the symmetrical U-shaped diurnal trend for NEE and GPP, which closely mirrored that of PAR. Conversely, R_{eco} exhibited a strong positive association with Tair and Tsoil, which, similarly, governed the asymmetrical U-shaped diurnal trend for R_{eco}, which closely mirrors that of Tair and, to a lesser extent, Tsoil.

At the daily timescale, the negative association between NEE fluxes and PAR weakened, offset by a stronger negative association with Tsoil. This mirrored GPP, which also exhibited a strong association with Tair. Daily R_{eco} remained largely consistent with half-hourly associations. Under snow-free conditions, VPD shared a moderate linear association with all CO_2

https://doi.org/10.5194/egusphere-2026-4164
Preprint. Discussion started: 28 August 2026

fluxes at both half-hourly and daily timescales. Conversely, WS, RH, and PPT exhibited indistinguishable linear associations with CO_2 fluxes. Under snow-covered conditions, the strength of linear associations between meteorological predictors and CO_2 fluxes substantially weakened, signifying a diminished influence of meteorological variables under snow-covered conditions.

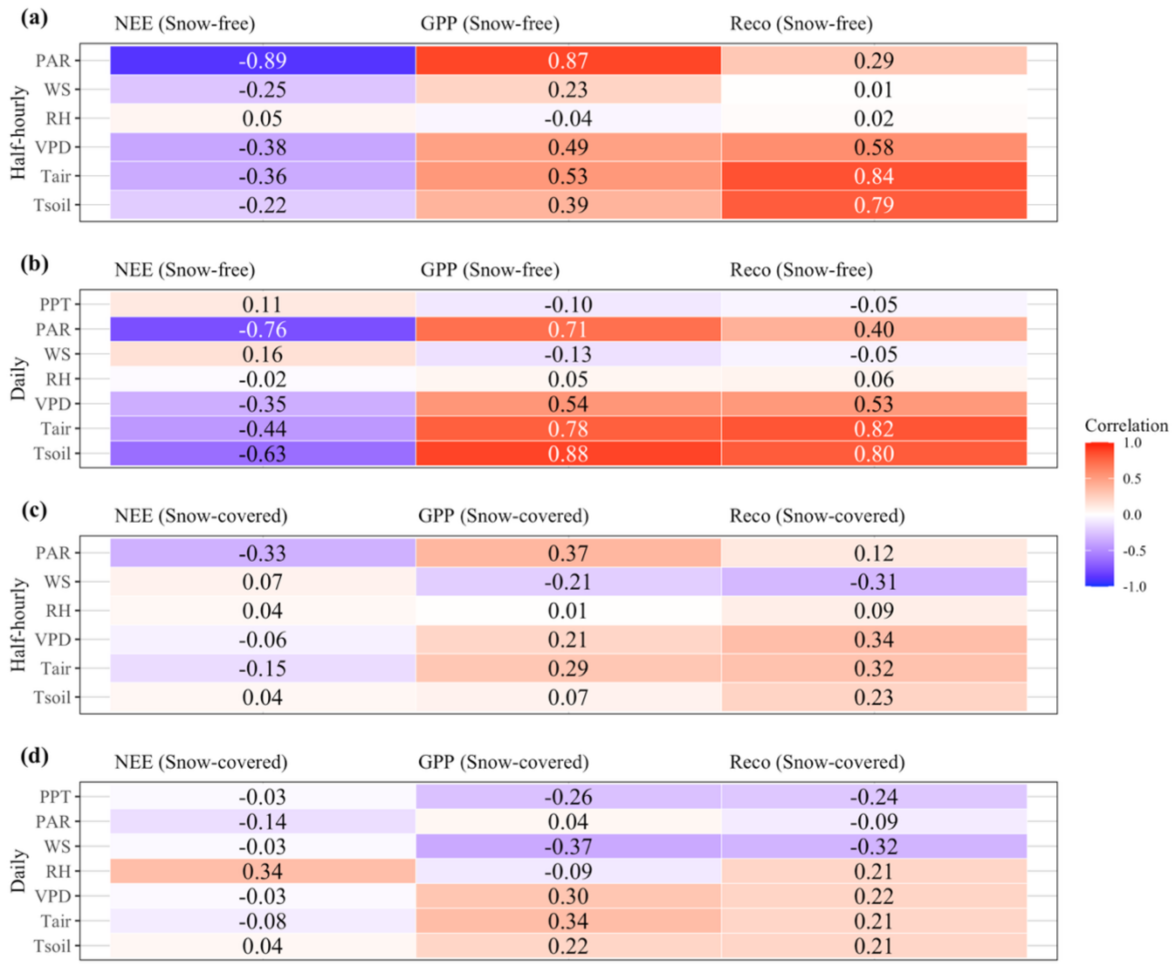

Fig. 5. Pearson correlation matrix between meteorological predictors of CO_2 fluxes under snow-free conditions at (a) half-hourly and (b) daily timescales, and under snow-covered conditions at (c) half-hourly and (d) daily timescales.

Fig. 6 presents the RF variable importance scores of meteorological predictors of CO_2 fluxes under snow-free and snow-covered conditions at half-hourly and daily timescales.

Under snow-free conditions, half-hourly NEE and GPP fluxes were most strongly predicted by PAR, followed by Tsoil, with RH, Tair, WS, and VPD returning comparatively low scores. Conversely, half-hourly R_{eco} was more equally predicted across all predictors, with RH exhibiting the highest score, followed by WS, Tsoil, PAR, Tair, and VPD.

https://doi.org/10.5194/egusphere-2026-4164
Preprint. Discussion started: 28 August 2026

Under snow-free conditions, daily NEE remained most strongly predicted by PAR, followed by Tsoil and Tair. GPP was most strongly predicted by Tsoil, followed by PAR and Tair, while R_{eco} was primarily predicted by Tsoil and Tair.

Under snow-covered conditions, the RF models for half-hourly NEE and GPP, as well as all daily CO_2 fluxes, returned comparatively low importance scores relative to snow-free conditions. This aligned with the percentage of variance in CO_2 fluxes explained by each RF model (Supplementary material). Under snow-free conditions, RF models explained substantial variance in half-hourly CO_2 fluxes, and to a lesser extent, daily CO_2 fluxes. This suggests the meteorological predictors PAR, Tsoil, RH, Tair, WS, VPD, and PPT were key predictors of diurnal and seasonal variances in CO_2 fluxes under snow-free conditions. Conversely, under snow-covered conditions, RF models explained minimal variance for both half-hourly and daily CO_2 fluxes, with the exclusion of half-hourly R_{eco}. This suggests that these meteorological predictors have diminished influence on the diurnal and seasonal variances of CO_2 fluxes under snow-covered conditions, aligning with the results of the Pearson correlation matrix.

Interestingly, the RF model for half-hourly R_{eco} explained substantial variance under snow-covered conditions, with variable rankings largely consistent with snow-free conditions, excluding PAR, which transitioned from the fourth to the least important variable.

https://doi.org/10.5194/egusphere-2026-4164
Preprint. Discussion started: 28 August 2026

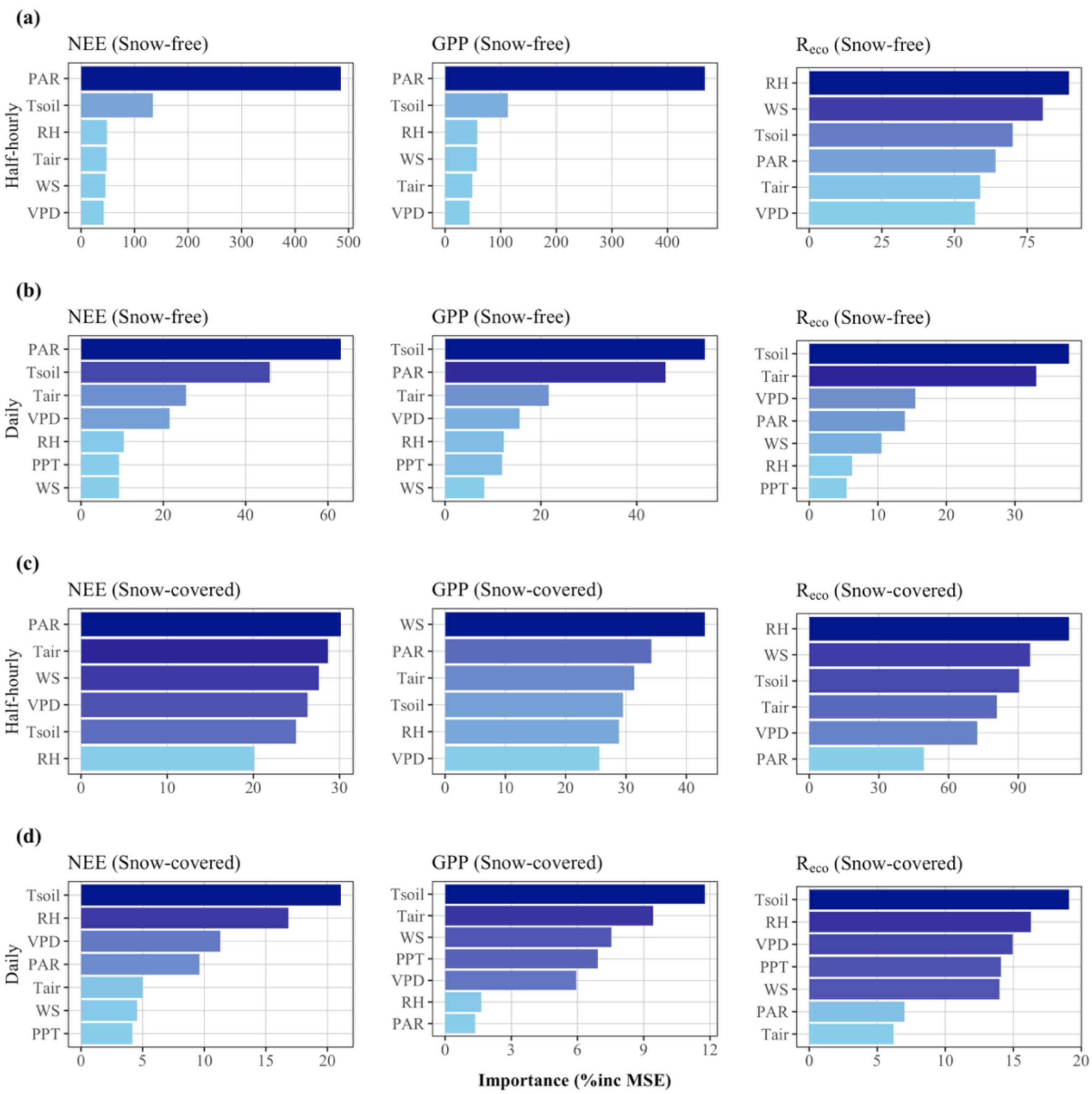

325 **Fig. 6.** Bar plots of RF variable importance for meteorological predictors on CO_2 fluxes under snow-free conditions at (a) half-hourly and (b) daily timescales, and under snow-covered conditions at (c) half-hourly and (d) daily timescales.

The partial dependence plots derived from the GAMs, depicting the relationships between meteorological variables PAR, Tsoil, and RH and NEE at half-hourly and daily timescales under snow-free and snow-covered conditions, are presented in Fig. 7. Under snow-free conditions, half-hourly NEE exhibited a strong, slightly exponential, negative relationship with PAR. This relationship is indicative of a typical photosynthetic light-response curve, where NEE decreases rapidly with the initial influx of PAR before gradually reaching a saturation point, where additional PAR yields diminishing NEE. At the daily

https://doi.org/10.5194/egusphere-2026-4164
Preprint. Discussion started: 28 August 2026

timescale, this relationship became more linear, with a smaller PAR range inhibiting the formation of a complete saturation trend. This relationship is consistent with the RF variable importance scores, with the negative relationship confirming the dominant influence of PAR on GPP relative to R_{eco}, driving net carbon influx.

Alternatively, Tsoil exhibited an asymmetrical U-shaped relationship with NEE across both half-hourly and daily timescales. This association is analogous to a thermal performance curve, wherein NEE declines exponentially from 0 °C to approximately 12-13 °C, before rising with subsequent temperature rises. Thus, 0 °C to 12-13 °C corresponds to a temperature range where increases in Tsoil correspond to a rise of net carbon influx, whilst subsequent temperature increase drives net carbon efflux.

Half-hourly RH shared an asymmetrical, inverted U-shaped relationship with NEE. Comparable to Tsoil, this relationship somewhat resembles a thermal performance curve, where NEE rapidly increases with RH between 0 % and approximately 25 %, gradually declines between 25 % and 75 %, before reverting to a gradual incline with additional increases. Similar to PAR, this is consistent with the RF variable importance scores, with a mostly positive relationship between NEE and RH confirming the dominant influence of RH on R_{eco} driving carbon efflux. At the daily timescale, there is no distinguishable relationship between NEE and RH evidenced by the underfitted partial dependence plot, which is consistent with the RF model.

Under snow-covered conditions, the relationships between NEE and PAR, Tsoil, and RH weakened with underfitted plots for daily PAR and RH and overfitted plots for half-hourly and daily Tsoil plots, signifying a weaker underlying signal-to-noise ratio. Half-hourly PAR, whilst exhibiting some overfitting, demonstrated a weaker negative relationship between NEE and PAR under snow-covered conditions, aligning with the results of the Pearson correlation and RF model. RH and NEE appear to maintain a relationship under snow-covered conditions, though varying from that exhibited under snow-free conditions. Between 0 % and approximately 35 %, NEE was negatively associated with RH, transitioning to a positive relationship between approximately 35 % and 60 %, before reverting to a negative association with higher RH.

https://doi.org/10.5194/egusphere-2026-4164
Preprint. Discussion started: 28 August 2026

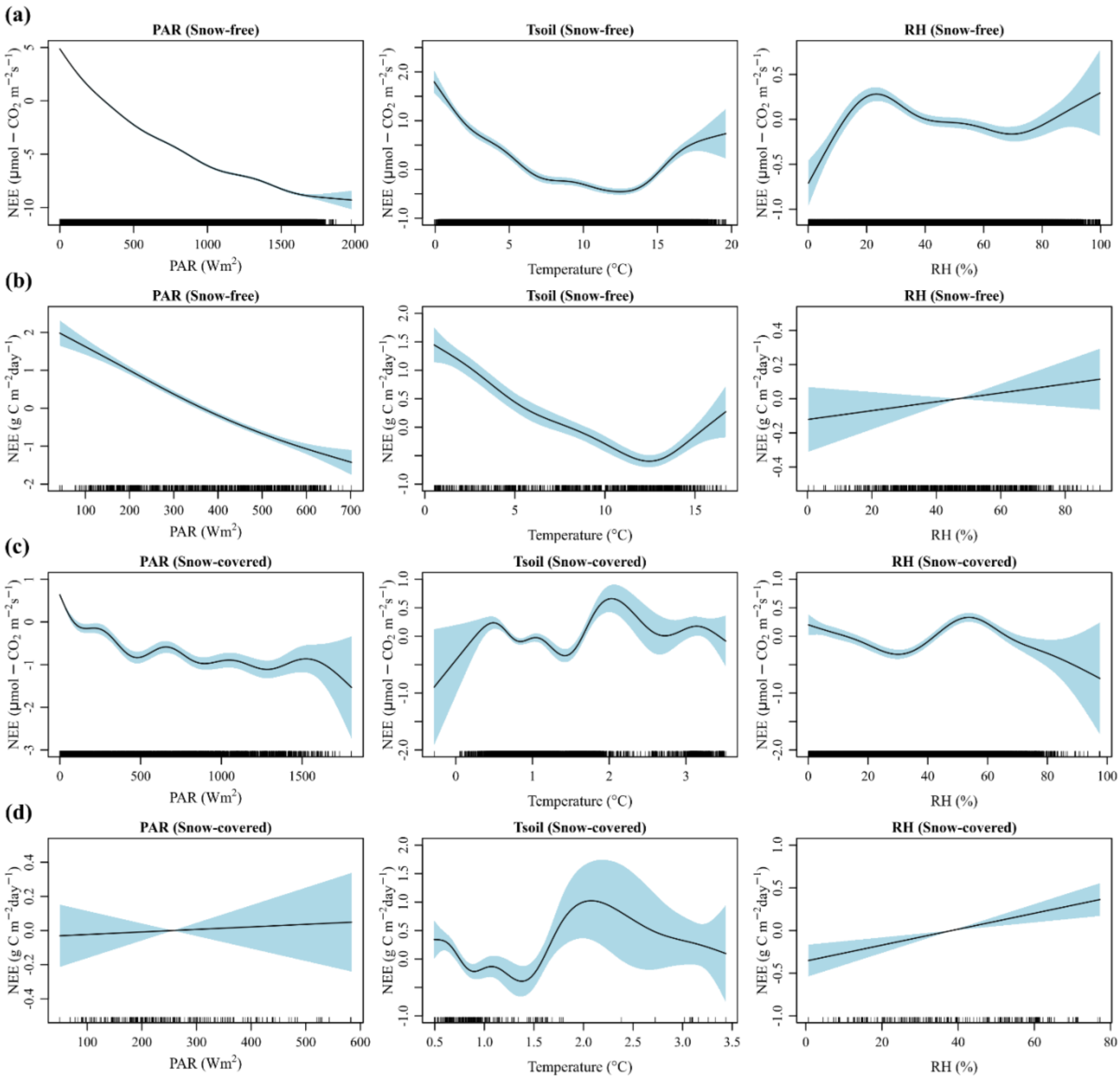

Fig. 7. Partial dependence plots derived from GAMs depicting the influence of meteorological variables on NEE under snow-free conditions at (a) half-hourly and (b) daily timescales, and under snow-covered conditions at (c) half-hourly and (d) daily timescales. Blue shaded areas correspond to a 95 % confidence interval.

https://doi.org/10.5194/egusphere-2026-4164
Preprint. Discussion started: 28 August 2026

5.0 Discussion

5.1 Influence of snow on GPP

The suppression of GPP under snow-covered conditions is primarily driven by the attenuation of PAR due to increased surface albedo and extinction within the snowpack. Statistical analysis of meteorological predictors of CO_2 fluxes demonstrated that PAR principally governed NEE and GPP under snow-free conditions. Under snow-covered conditions, the strength of these associations substantially diminished. This is consistent with observations made by Zhao et al (2010), over an alpine meadow in the Tibetan Plateau, where the dominant influence of PAR on daily variations in NEE was confined to the growing season. The heightened surface albedo associated with the snowpack at the study site is depicted in Fig. 8, where steep declines in net shortwave radiation (K*) coincide with the formation of the snowpack. Under snow-free conditions, mean K* was 314.87 Wm^{-2}, decreasing to 80.12 Wm^{-2} under snow-covered conditions. Of this, Körner (2021) notes the remaining irradiance would be adsorbed or backscattered within the first 30 cm of the snowpack, leaving marginal PAR to sustain photosynthetic activity. Despite this, autotrophs at our site continued photosynthesising under shallow snow-covered conditions, indicated by a slight decrease in NEE during daytime hours in Fig. 4. Ultimately, the attenuation of PAR by the deeper snowpack largely inhibited photosynthesis, transitioning the site to a net carbon source, aided by the subsequent insulating of the underlying ground.

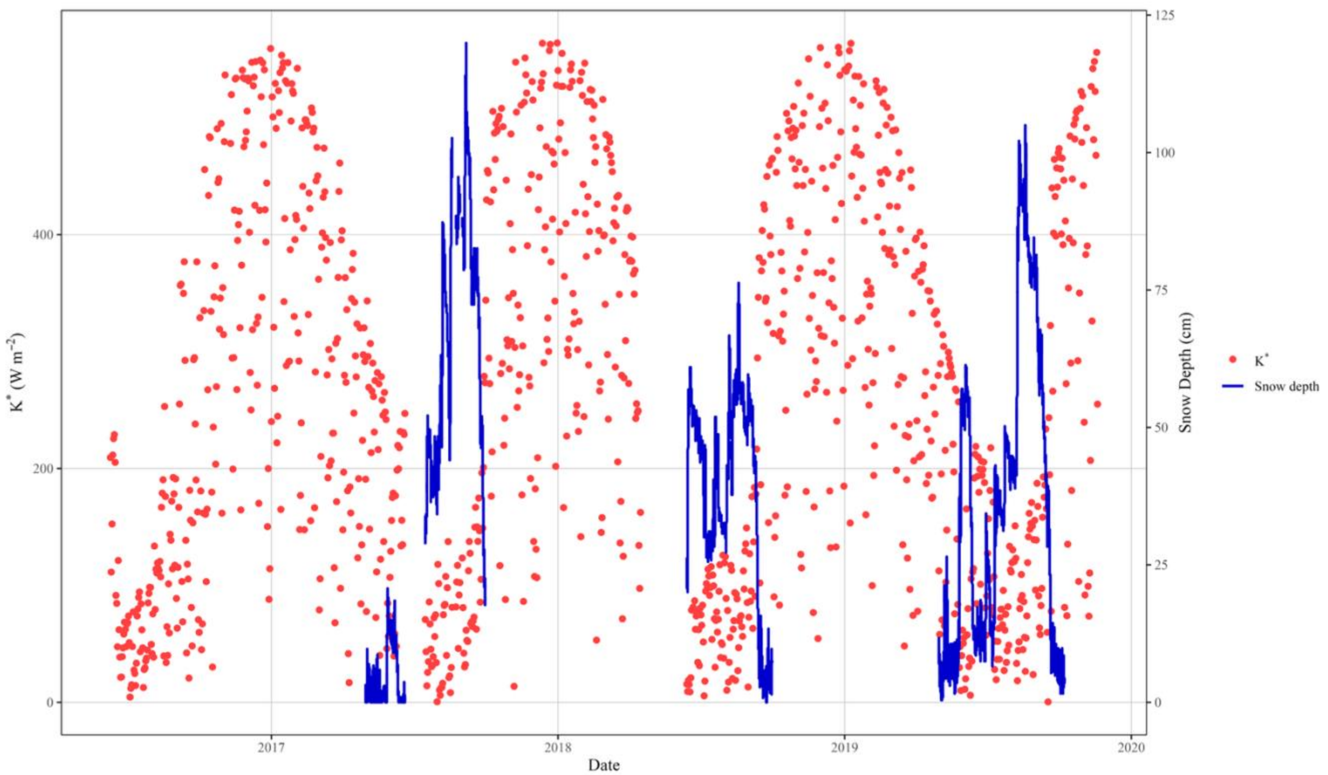

Fig. 8. Prevailing net shortwave radiation (K^*) overlaid with snow depth.

https://doi.org/10.5194/egusphere-2026-4164
Preprint. Discussion started: 28 August 2026

5.2 Influence of snow on R_{eco}

Persistent R_{eco} under snow-covered conditions can be largely attributed to the insulation of the underlying soil by the snowpack, modulating Tsoil. A timeseries of meteorological variables presented in Fig. 4 depicts Tsoil closely mirroring seasonal variations in Tair, except during periods of snow cover, where it plateaus between 0℃ and 2℃. This is reinforced in Fig. 9, where the close positive linear association between Tair and Tsoil under snow-free conditions dissociates under snow-covered conditions. It has been widely established in literature that the low thermal conductivity of snowpacks insulates the underlying ground, maintaining a soil temperature threshold that facilitates both plant and soil respiration (Körner 2021, Warren and Taranto 2011, Zhang 2005). This phenomenon has been observed at the study site where the plateauing of Tsoil coincides with the persistence of R_{eco} under snow-covered conditions depicted in Figs. 3 and 4. Additionally, the insulating influence of the snowpack likely prevented freeze-thaw events and associated drops in respiration (Warren and Taranto, 2011; Sorensen et al., 2018).

Notably, the RF model of half-hourly R_{eco} indicated all meteorological variables, excluding PAR, similarly influenced R_{eco} under snow-free and snow-covered conditions, suggesting the influence of these meteorological variables on the diurnal variations of R_{eco} was not perturbed by the snowpack. This seems unlikely given that the snowpack would likely shield the underlying ground from diurnal oscillations in RH, WS, Tair, and VPD. Thus, the insulation of ground temperatures facilitated by the snowpacks remains the dominant mechanism driving persistent R_{eco} under snow-covered conditions, transitioning the site from a net carbon sink to a source under snow-covered conditions.

Analysis on the influence of snow on both GPP and R_{eco} was limited by the exclusion of important meteorological and biological parameters, which were not observed as part of this study. These include, but are not limited to, soil water content, leaf area index, and substrate availability, all of which have been observed as key predictors of NEE fluxes in snow-covered ecosystems (Koch et al., 2008; Zhao et al., 2010). In excluding such predictors, the strength of associations between the selected predictors and CO_2 fluxes is likely inflated, overestimating their relative importance in determining diurnal and seasonal variances of CO_2 fluxes.

https://doi.org/10.5194/egusphere-2026-4164
Preprint. Discussion started: 28 August 2026

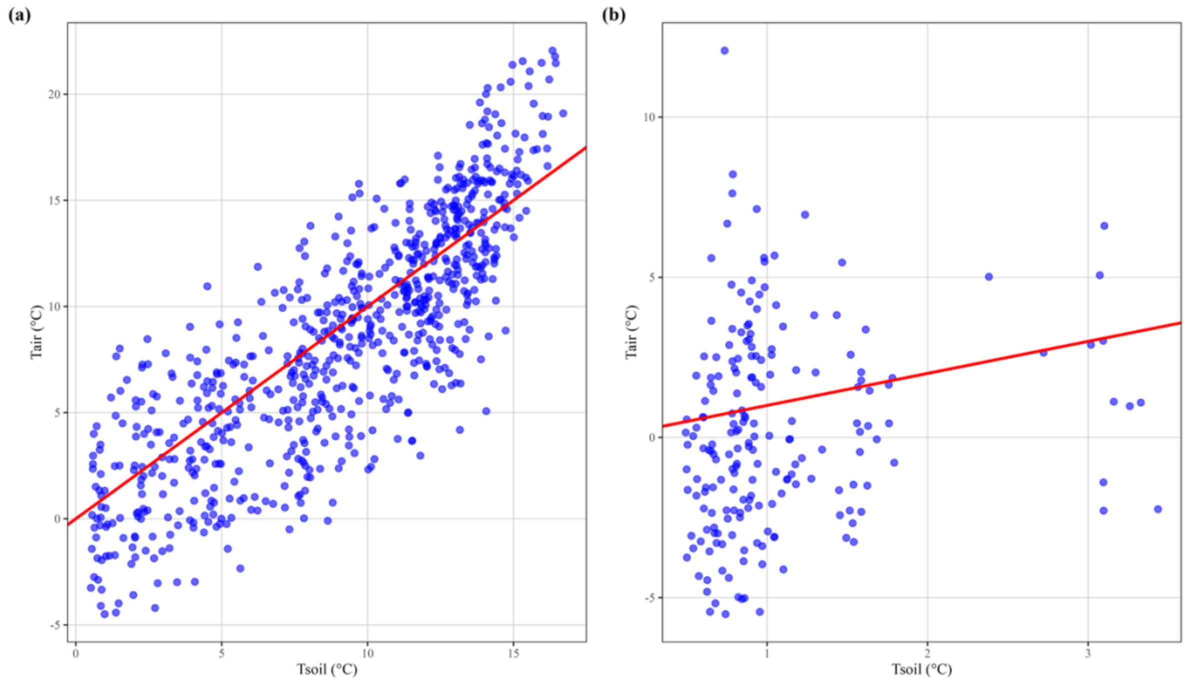

Fig. 9. Tsoil and Tair (a) under snow-free conditions and (b) under snow-covered conditions; the red line denotes the 1:1 line.

5.3 Comparison of NEE over other alpine meadow communities

The seasonality of CO_2 fluxes at the study site saw the site function as a net carbon sink under snow-free conditions and a net carbon source under snow-covered conditions. This is consistent with NEE over most alpine meadow systems, with comparable CO_2 flux timeseries and cumulative plots presented in Zhao et al (2010) and Knowles et al (2019). Likewise, seasonality in NEE has been observed in other alpine communities. Reverter et al (2010) noted the dominance of R_{eco} during snow-covered conditions over an alpine shrubland community, which changed the system from a net carbon sink. Similarly, Gunawardhana et al (2025) observed the transition of a peatland community in the Australian Alps from a net carbon sink under snow-free conditions to a net carbon source under snow-covered conditions. Table 2 presents the annual CO_2 fluxes recorded at the study site alongside those observed in other alpine meadow communities globally.

The study site functioned as a strong net carbon sink relative to other alpine meadow communities, with considerably higher GPP and R_{eco} fluxes. More broadly, the ecosystem functioned as a strong net carbon sink relative to other ecosystems, with Baldocchii (2014) reporting the mean of -156 +- 284 gC m^{-2} yr^{-1} across approximately 1400 sites, with the most negative values associated with evergreen plantations and positive values associated with disturbed sites (Baldocchi, 2014). The strength of the net carbon sink corresponds with the prevailing climate, which facilitates a comparatively short snow-covered period that enables the site to function as a net carbon sink for longer. This is consistent with Gunawardhana et al. (2025), who observed a comparatively strong net carbon sink over peatland systems of the Australian Alps, relative to those in the Northern Hemisphere. Likewise, Warren and Taranto (2011) noted that below-snow R_{eco} contributed little to annual R_{eco} in a sub-alpine

https://doi.org/10.5194/egusphere-2026-4164
Preprint. Discussion started: 28 August 2026

grassland ecosystem in the Australian Alps due to the comparatively short snow season. They observed below snow R_{eco} contributed 4.1-4.3 % of annual R_{eco}, which is lower than the 13.08 % recorded at the study sites. Regardless, both systems recorded values lower than those of comparable ecosystems in the Northern Hemisphere, with longer snow seasons (10-50 %) (Warren and Taranto, 2011). Thus, the comparatively long snow-free period enables alpine meadow ecosystems in the Australian Alps to sequester comparatively higher levels of carbon, relative to their Northern Hemisphere counterparts. In doing so, it reinforces the value of these systems in offsetting carbon emitted to the atmosphere from anthropogenic sources as well as the urgency of conserving and managing these areas accordingly.

https://doi.org/10.5194/egusphere-2026-4164
Preprint. Discussion started: 28 August 2026

Table 2. Annual CO_2 fluxes of other alpine meadow communities.

Ecosystem	Location	Elevation (m)	Longitude/ Latitude	Survey period	NEE	GPP	R_{eco}	Reference
Alpine meadow	Australian Alps	1847	36.42° S / 148.42° E	2016-2019	-216.9	1183.5	966.6	Present study
Tropical alpine grassland	Northern Andean Páramo	3765	3.06° S / 79.24° W	2016-2018	98.8	1170.8	1269.5	Carrillo-Rojas et al., 2019
Alpine tundra	Rocky Mountains	3050	40.05° N / 105.59° W	2008-2012	232.4	108.6	341.0	Knowles et al., 2019
Alpine wet meadow	Qinghai-Tibetan Plateau	3250	37.58° N / 101.33° E	2004-2006	106.1	629.9	737.3	Zhao et al., 2010
Alpine meadow	Italian Alps	1550	46.01° N / 11.04° E	2003-2009	-9.1	-	-	Marcolla et al., 2011
Alpine meadow	Tibetan Plateau	3033	38.05° N / 100.46° E	2015-2016	-198.9	818.3	619.6	Sun et al., 2019
Alpine meadow	Tibetan Plateau	3739	38.84° N / 98.94° E	2015-2016	-258.9	467.5	208.6	Sun et al., 2019
Alpine meadow	Tibetan Plateau	4148	38.01° N / 100.24° E	2015-2016	-105.3	228.6	123.3	Sun et al., 2019
Alpine peatland	Italian Alps	1563	46.02° N / 11.04° E	2012-2014	180.7	1191	1307.7	Pullen et al., 2016
Sub-alpine peatland	Australian Alps	1670-1750	36.86° S / 147.32° E	2017-2019	-320.6	1198.3	877.7	Gunawardhana et al. 2025

https://doi.org/10.5194/egusphere-2026-4164
Preprint. Discussion started: 28 August 2026

5.3 CO_2 flux and climate change

Literature on NEE over alpine meadows under future climate regimes is univocal. Alpine grasslands on the Tibetan Plateau have exhibited a stronger net carbon sink of 1.14 tg C year^{-1} between 1982 and 2018, largely derived from an increased temperature environment (Wang et al., 2023). Conversely, alpine tundra communities on the Niwot Ridge in Colorado have shown a stronger net carbon source resulting from permafrost thawing under warmer soil temperatures (Knowles et al., 2019). Warmer temperatures, reduced winter precipitation, and higher rates of snowmelt are anticipated to reduce the temporal and spatial extent of snowpacks in the Australian Alps by 15 % by 2030 and 60% by 2070 (Di Luca et al., 2018). This will increase the snow-free period and, therefore, the period during which the system functions as a net carbon sink, assuming ecosystem dynamics remain constant. Similar conclusions have been considered by Pullens et al. (2016) and Humphreys and Lafleur (2011), both acknowledging the fragility of such conclusions given the complex interactions between environmental drivers. The GAM between NEE and Tsoil presented in Fig. 7 for both half-hourly and daily timescales depicted a positive relationship between NEE and Tsoil beyond approximately 12-13 ℃, signifying a threshold where additional increases in soil temperature promote carbon efflux. This suggests that warmer soil temperatures under future climate regimes may accelerate R_{eco}, particularly if not offset by proportionate increases in PAR to sustain comparable increases in GPP, which is unlikely. Thus, there is potential that the additional carbon sequestered under longer snow-free periods could be subsequently lost by increased R_{eco} under warmer soil temperatures, particularly under high temperature extremes experienced during summer months. This aligns with Saito et al. (2009), who noted that the sink strength of an alpine meadow community on the Tibetan Plateau would decrease under warmer conditions, without comparable increases in PAR under future climate regimes.

6.0 Conclusion

As climate change continues unabated, it is pivotal to understand the NEE of vulnerable ecosystems. Here we have presented results from the first direct measurement of CO_2 fluxes over a distinct alpine meadow ecosystem in the Australian Alps using EC. CO_2 fluxes for the site exhibited strong seasonality, functioning as a net carbon sink under snow-free conditions, before transitioning to a net carbon source under snow-covered conditions. This seasonal variation was predominantly driven by the attenuation of PAR inhibiting GPP and insulation of Tsoil sustaining R_{eco} under snow-covered conditions. Despite the marginal nature of the Australian snowpack, NEE under snow-covered conditions was consistent with that of other alpine meadow ecosystems associated with deeper snowpacks. The system functioned as a strong net carbon sink, sequestering an average of 216.9 g C m^2 yr^{-1} annually, across the three-year study period. CO_2 fluxes were greater relative to other alpine meadow systems, globally, largely resulting from a comparatively shorter snow-covered period. As the spatial and temporal extent of snowpacks in the Australian Alps is anticipated to decrease under future climate regimes, it is anticipated that the sink strength of alpine meadow communities in the Australian Alps will increase. However, associated soil temperature increases may accelerate R_{eco}, which could offset additional carbon sequestration from a longer snow-free period. Additional long-term EC data from

https://doi.org/10.5194/egusphere-2026-4164
Preprint. Discussion started: 28 August 2026

representative alpine meadow ecosystems is required to establish long-term relationships between environmental drivers and CO_2 fluxes, thereby guaranteeing more accurate NEE modelling to inform improved management practices and policy decisions. Additionally, it is recommended that alpine meadow communities and comparable ecosystems in the Australian Alps be conserved and managed effectively to preserve their value in offsetting carbon emitted to the atmosphere from anthropogenic sources

https://doi.org/10.5194/egusphere-2026-4164
Preprint. Discussion started: 28 August 2026

Appendix A. Diurnal CO_2 fluxes

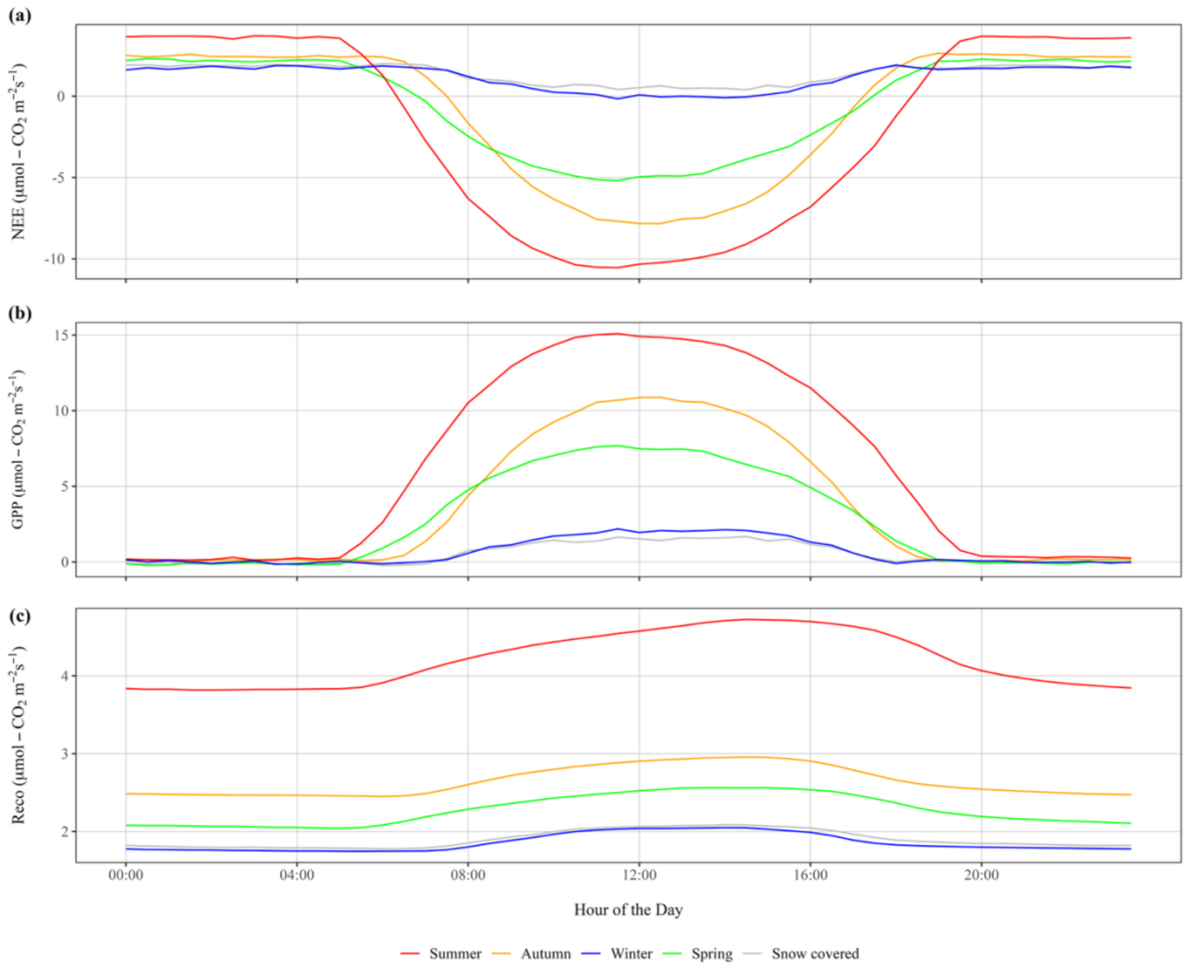

Fig. A1. Diurnal CO_2 fluxes for summer, autumn, winter, spring, and snow-covered conditions, (a) NEE, (b) GPP, (C) R_{eco}.

465

https://doi.org/10.5194/egusphere-2026-4164
Preprint. Discussion started: 28 August 2026

470 **Appendix B. Predictive performance of statistical models**

Table B1. Percentage of variance explained by random forest and generalised additive models.

Flux	Timescale	Condition	Percentage explained (%)
		Random Forest Model	
NEE	Half-hourly	Snow-free	84.77
GPP	Half-hourly	Snow-free	86.67
R_{eco}	Half-hourly	Snow-free	83.28
NEE	Daily	Snow-free	76.20
GPP	Daily	Snow-free	88.20
R_{eco}	Daily	Snow-free	74.78
NEE	Half-hourly	Snow-covered	17.22
GPP	Half-hourly	Snow-covered	30.20
R_{eco}	Half-hourly	Snow-covered	75.63
NEE	Daily	Snow-covered	34.43
GPP	Daily	Snow-covered	21.61
R_{eco}	Daily	Snow-covered	39.88
		Generalised Additive Model	
NEE	Half-hourly	Snow-free	81.9
NEE	Daily	Snow-free	66.9
NEE	Half-hourly	Snow-covered	17.2
NEE	Daily	Snow-covered	27.9

Code and data availability

Data pertaining to this study is available at:

Scott, Samuel and McGowan, Hamish.: Pipers Creek alpine CO2 flux and meteorological data, Snowy Mountains, Australia,
475 The University of Queensland, Data Collection, https://doi.org/10.48610/26bb8f3, 2026.

https://doi.org/10.5194/egusphere-2026-4164
Preprint. Discussion started: 28 August 2026

Author contributions

HM designed the field experiment and oversaw data collection at the study site. SS designed the data processing and statistical analysis methodology and prepared subsequent model codes, figures, and manuscript with contributions from HM.

Competing interests

The authors declare that they have no known competing financial interests or personal relationships that could have appeared to influence the work reported in this paper.

Acknowledgements

The authors thank Michael Gray, Andrew Schwartz, Nik Callow and Shane Bilish for their assistance with the installation, maintenance, data collection, and management of the Pipers Creek eddy covariance tower. We also acknowledge the support of Snowy Hydro Ltd. and the New South Wales National Parks and Wildlife Service. Colin de Pagter from HeliSurveys is thanked for his assistance in the field during the installation and decommissioning of the eddy covariance tower and ancillary snow pack monitoring.

Financial support

Snowy Hydro Ltd. provided the funding for this research through research contract #91085 to The University of Queensland.

References

Baldocchi, D. D.: Assessing the eddy covariance technique for evaluating carbon dioxide exchange rates of ecosystems: past, present and future, Glob. Change Biol., 9, 479–492, https://doi.org/10.1046/j.1365-2486.2003.00629.x, 2003.

Bilish, S. P., McGowan, H. A., and Callow, J. N.: Energy balance and snowmelt drivers of a marginal subalpine snowpack, Hydrol. Process., 32, 3837–3851. https://doi.org/10.1002/hyp.13293, 2018.

Bilish, S. P., Callow, J. N., McGrath, G. S., and McGowan, H. A.: Spatial controls on the distribution and dynamics of a marginal snowpack in the Australian Alps, Hydrol. Process., 33, 1739–1755. https://doi.org/10.1002/hyp.13435, 2019.

Breiman, L.: Random Forests, Mach. Learn., 45, 5–32, https://doi.org/10.1023/A:1010933404324, 2001.

Carrillo-Rojas, G., Silva, B., Rollenbeck, R., Célleri, R., and Bendix, J.: The breathing of the Andean highlands: Net ecosystem exchange and evapotranspiration over the páramo of southern Ecuador, Agric. For. Meteorol., 265, 30–47, https://doi.org/10.1016/j.agrformet.2018.11.006, 2019.

Chubb, T. H., Siems, S. T., and Manton, M. J.: On the Decline of Wintertime Precipitation in the Snowy Mountains of Southeastern Australia, J. Hydrometeorol., 12, 1483–1497. https://doi.org/10.1175/JHM-D-10-05021.1, 2011.

Costin, A., Gray, M., Totterdell, C., and Wimbush, D.: Kosciuszko Alpine flora, 2nd ed., CSIRO Publishing, Collingwood, Victoria, 2000.

Connell Wagner Pty Ltd.: Perisher Range Resorts Environmental Study: Report prepared for NSW National Parks and Wildlife Service, Connell Wagner Pty Ltd., Neutral Bay, New South Wales, 2000.

Department of Climate Change, Energy, the Environment and Water: National heritage places – Australian Alps National Parks and Reserves, https://www.dcceew.gov.au/parks-heritage/heritage/places/national/australia-alps, last accessed: 10 November 2023.

Falge, E., Baldocchi, D., Olson, R., Anthoni, P., Aubinet, M., Bernhofer, C., Burba, G., Ceulemans, R., Clement, R., Dolman, H., Granier, A., Gross, P., Grünwald, T., Hollinger, D., Jensen, N.-O., Katul, G., Keronen, P., Kowalski, A., Ta Lai, C., et al.: Gap filling strategies for long term energy flux data sets, Agric. For. Meteorol., 107, 71–77, https://doi.org/10.1016/S0168-1923(00)00235-5, 2001a

Falge, E., Baldocchi, D., Olson, R., Anthoni, P., Aubinet, M., Bernhofer, C., Burba, G., Ceulemans, R., Clement, R., Dolman, H., Granier, A., Gross, P., Grünwald, T., Hollinger, D., Jensen, N.-O., Katul, G., Keronen, P., Kowalski, A., Lai, C. T., et al.: Gap filling strategies for defensible annual sums of net ecosystem exchange, Agric. For. Meteorol.,107, 43–69. https://doi.org/10.1016/S0168-1923(00)00225-2, 2001b.

Ecology Australia Pty Ltd: Kosciuszko Resorts Vegetation Assessment: Report prepared for Planning NSW, Ecology Australia Pty Ltd, Fairfield, Victoria, 2003.

Gray, M. A., McGowan, H. A., Lowry, A. L., and Guyot, A.: Surface energy exchanges over contrasting vegetation types on a sub-tropical sand island, Agric. For. Meteorol., 249, 81–99, https://doi.org/10.1016/j.agrformet.2017.11.018, 2018.

Gunawardhana, M., Treby, S., Silvester, E., Callesen, T. O., Jones, O. A. H., and Grover, S.: Intact Australian Sphagnum peatland is a strong carbon sink, Sci. Total Environ., 959, Article 178197, https://doi.org/10.1016/j.scitotenv.2024.178197, 2025.

Hastie, T., and Tibshirani, R.: Generalized Additive Models, Stat. Sci., 1, 297–310, https://doi.org/10.1214/ss/1177013604, 1986.

Hubbard, R. M., Ryan, M. G., Elder, K., and Rhodes, C. C.: Seasonal patterns in soil surface CO_2 flux under snow cover in 50 and 300 year old subalpine forests, Biogeochemistry, 73, 93–107, 2005.

Humphreys, E. R., and Lafleur, P. M.: Does earlier snowmelt lead to greater CO2 sequestration in two low Arctic tundra ecosystems?, Geophys. Res. Lett., 38, https://doi.org/10.1029/2011GL047339, 2011.

Kljun, N., Calanca, P., Rotach, M. W., and Schmid, H. P.: The simple two-dimensional parameterisation for Flux Footprint Prediction (FFP), Geosci. Model Dev., 8, 3695–3713, https://doi.org/10.5194/gmd-8-3695-2015, 2015.

Knowles, J. F., Burns, S. P., Blanken, P. D., and Monson, R. K.: Fluxes of energy, water, and carbon dioxide from mountain ecosystems at Niwot Ridge, Colorado, Plant Ecol. Divers., 8, 663–676, https://doi.org/10.1080/17550874.2014.904950, 2015.

Knowles, J. F., Blanken, P. D., Lawrence, C. R., and Williams, M. W.: Evidence for non-steady-state carbon emissions from snow-scoured alpine tundra, Nat. Commun., 10, Article 1306. https://doi.org/10.1038/s41467-019-09149-2, 2019.

Koch, O., Tscherko, D., Küppers, M., and Kandeler, E.: Interannual Ecosystem CO_2 Dynamics in The Alpine Zone of The Eastern Alps, Austria, Arct. Antarct. Alp. Res., 40, 487–496. https://doi.org/10.1657/1523-0430(07-055)[KOCH]2.0.CO;2, 2008.

Körner, C.: Alpine Plant Life: Functional Plant Ecology of High Mountain Ecosystems, 3rd ed., Springer International Publishing, https://doi.org/10.1007/978-3-030-59538-8, 2021.

Liaw, A., and Wiener, M.: Classification and regression by randomForest, R News, 2, 18–22, 2002.

Liu, J., and van Iersel, M. W.: Photosynthetic Physiology of Blue, Green, and Red Light: Light Intensity Effects and Underlying Mechanisms, Front. Plant Sci., 12, 619987, https://doi.org/10.3389/fpls.2021.619987, 2021.

Lloyd, J., and Taylor, J. A.: On the Temperature Dependence of Soil Respiration, Funct. Ecol., 8, 315–323, https://doi.org/10.2307/2389824, 1994.

Luca, A. D., Evans, J. P., and Ji, F.: Australian snowpack in the NARCliM ensemble: evaluation, bias correction and future projections, Clim. Dyn., 51, 639–666. https://doi.org/10.1007/s00382-017-3946-9, 2018.

Ma, W., Wu, T., Wu, X., Yang, S., Li, R., Zhou, S., Li, X., Zhu, X., Hao, J., Ni, J., and Wang, D.: Carbon budgets and environmental controls in alpine ecosystems on the Qinghai-Tibet Plateau, Catena, 229, Article 107224, https://doi.org/10.1016/j.catena.2023.107224, 2023.

MacDougall, A. S., Vanzant, B., Sulik, J., Bagchi, S., Naidu, D., Muraina, T. O., Seabloom, E. W., Borer, E. T., Wilfahrt, P., Slette, I., Hierro, J. L., Pearson, D. E., Abedi, M., Akasaka, M., Anderson, T. M., Arnillas, C. A., Ayer, M., Basto, S., Biederman, L., et al.: The global extent of the grassland biome and implications for the terrestrial carbon sink, Nat. Ecol. Evol., 10, 246–257, https://doi.org/10.1038/s41559-025-02955-6, 2026.

Marcolla, B., Cescatti, A., Manca, G., Zorer, R., Cavagna, M., Fiora, A., Gianelle, D., Rodeghiero, M., Sottocornola, M., and Zampedri, R.: Climatic controls and ecosystem responses drive the inter-annual variability of the net ecosystem exchange of an alpine meadow, Agric. For. Meteorol., 15, 1233–1243. https://doi.org/10.1016/j.agrformet.2011.04.015, 2011.

McCree, K. J.: The action spectrum, absorptance and quantum yield of photosynthesis in crop plants, Agric. Meteorol., 9, 191–216, https://doi.org/10.1016/0002-1571(71)90022-7, 1972.

Merbold, L., Rogiers, N., and Eugster, W.: Winter CO_2 fluxes in a sub-alpine grassland in relation to snow cover, radiation and temperature, Biogeochemistry, 111, 287–302, https://doi.org/10.1007/s10533-011-9647-2, 2012.

https://doi.org/10.5194/egusphere-2026-4164
Preprint. Discussion started: 28 August 2026

Monson, R. K., Lipson, D. L., Burns, S. P., Turnipseed, A. A., Delany, A. C., Williams, M. W., and Schmidt, S. K.: Winter forest soil respiration controlled by climate and microbial community composition, Nature, 439, 711–714. https://doi.org/10.1038/nature04555, 2006.

Pal, A., and Chakravarty, A. K.: Genetics and breeding for disease resistance of livestock, 1st ed., Academic Press, an imprint of Elsevier, https://doi.org/10.1016/C2018-0-00046-8, 2020.

Papale, D., Reichstein, M., Aubinet, M., Canfora, E., Bernhofer, C., Kutsch, W., Longdoz, B., Rambal, S., Valentini, R., Vesala, T., and Yakir, D.: Towards a standardized processing of Net Ecosystem Exchange measured with eddy covariance technique: algorithms and uncertainty estimation, Biogeosciences, 3, 571–583, https://doi.org/10.5194/bg-3-571-2006, 2006.

Pullens, J. W. M., Sottocornola, M., Kiely, G., Toscano, P., and Gianelle, D.: Carbon fluxes of an alpine peatland in Northern Italy, Agric. For. Meteorol., 220, 69–82, https://doi.org/10.1016/j.agrformet.2016.01.012, 2016.

Reichstein, M., Falge, E., Baldocchi, D., Papale, D., Aubinet, M., Berbigier, P., Bernhofer, C., Buchmann, N., Gilmanov, T., and Granier, A.: On the separation of net ecosystem exchange into assimilation and ecosystem respiration: review and improved algorithm, Glob. Chang. Biol., 11, 1424–1439, https://doi.org/10.1111/j.1365-2486.2005.001002.x, 2005a.

Reichstein, M., Kätterer, T., Andrén, O., Ciais, P., Schulze, E.-D., Cramer, W., Papale, D., and Valentini, R.: Temperature sensitivity of decomposition in relation to soil organic matter pools: critique and outlook, Biogeosciences, 2, 317–321, https://doi.org/10.5194/bg-2-317-2005, 2005b.

Reichstein, M., Subke, J. A., Angeli, A. C., and Tenhunen, J. D.: Does the temperature sensitivity of decomposition of soil organic matter depend upon water content, soil horizon, or incubation time?, Glob. Change Biol., 11, 1754–1767, https://doi.org/10.1111/j.1365-2486.2005.001010.x, 2005c.

Reverter, B. R., Sánchez-Cañete, E. P., Resco, V., Serrano-Ortiz, P., Oyonarte, C., and Kowalski, A. S.: Analyzing the major drivers of NEE in a Mediterranean alpine shrubland, Biogeosciences, 7, 2601–2611, https://doi.org/10.5194/bg-7-2601-2010, 2010.

Robson, T. M., and Aphalo, P. J.: Transmission of ultraviolet, visible and near-infrared solar radiation to plants within a seasonal snow pack, Photochem. Photobiol. Sci., 18, 1963–1971, https://doi.org/10.1039/c9pp00197b, 2019.

Sahukar, R., Gallery, C., Smart, J., and Mitchell, P.: The bioregions of New South Wales: Their biodiversity, conservation and history, NSW National Parks and Wildlife Service, Hurstville, NSW, 2003.

Schwartz, A. J., McGowan, H., and Callow, N.: Impact of fire on montane snowpack energy balance in Snow Gum forest stands, Agric. For. Meteorol., 294, Article 108164, https://doi.org/10.1016/j.agrformet.2020.108164, 2020a.

Schwartz, A. J., McGowan, H. A., Theobald, A., and Callow, N.: Quantifying the impact of synoptic weather types and patterns on energy fluxes of a marginal snowpack, Cryosphere, 14, 2755–2774, https://doi.org/10.5194/tc-14-2755-2020, 2020b.

https://doi.org/10.5194/egusphere-2026-4164
Preprint. Discussion started: 28 August 2026

Schwartz, A., McGowan, H., and Callow, N.: Snowpack thermal patterns in pre- and post-bushfire Snow Gum forests, J. Hydrol., 602, Article 126789, https://doi.org/10.1016/j.jhydrol.2021.126789, 2021.

Schulze, E.-Detlef., and Caldwell, M. M. (Eds.): Ecophysiology of Photosynthesis, 1st ed, Springer Berlin Heidelberg, https://doi.org/10.1007/978-3-642-79354-7, 1995.

Saito, M., Kato, T., and Tang, Y.: Temperature controls ecosystem CO_2 exchange of an alpine meadow on the northeastern Tibetan Plateau, Glob. Change Biol., 15, 221–228, https://doi.org/10.1111/j.1365-2486.2008.01713.x, 2009.

Skinner, H.: Winter carbon dioxide fluxes in humid-temperate pastures, Agric. For. Meteorol., 144, 32–43, https://doi.org/10.1016/j.agrformet.2007.01.010, 2007.

Smith, M. W.: Microclimate influences on ground temperatures and permafrost distribution, Mackenzie Delta, Northwest Territories, Can. J. Earth Sci., 12, 1421–1438, 1975.

Snowy Hydro Ltd.: Snowy Hydro Limited Snow Depths Calculator, Snowy Hydro Ltd., Cooma, NSW, 2023.

Sorensen, P. O., Finzi, A. C., Giasson, M.-A., Reinmann, A. B., Sanders-DeMott, R., and Templer, P. H.: Winter soil freeze-thaw cycles lead to reductions in soil microbial biomass and activity not compensated for by soil warming, Soil Biol. Biochem., 116, 39–47, https://doi.org/10.1016/j.soilbio.2017.09.026, 2018.

Stern, H., de Hoedt, G., and Ernst, J.: Objective classification of Australian climates, Aust. Meteorol. Mag., 49, 87-96, 2000.

Stiperski, I., and Rotach, M. W.: Erratum to: On the Measurement of Turbulence Over Complex Mountainous Terrain, Bound.-Layer Meteorol., 161, 223–223, https://doi.org/10.1007/s10546-015-0115-8, 2016.

Sun, S., Che, T., Li, H., Wang, T., Ma, C., Liu, B., Wu, Y., and Song, Z.: Water and carbon dioxide exchange of an alpine meadow ecosystem in the northeastern Tibetan Plateau is energy-limited, Agric. For. Meteorol., 275, 283–295, https://doi.org/10.1016/j.agrformet.2019.06.003, 2019.

Theobald, A., McGowan, H., and Speirs, J.: Trends in synoptic circulation and precipitation in the Snowy Mountains region, Australia, in the period 1958–2012, Atmos. Res., 169, 434–448, https://doi.org/10.1016/j.atmosres.2015.05.007, 2016.

Euskirchen, E. S., Bret-Harte, M. S., Scott, G. J., Edgar, C., and Shaver, G. R.: Seasonal patterns of carbon dioxide and water fluxes in three representative tundra ecosystems in northern Alaska, Ecosphere, 3, 1-19, https://doi.org/10.1890/ES11-00202.1, 2012.

Vickers, D., and Mahrt, L.: Quality Control and Flux Sampling Problems for Tower and Aircraft Data, J. Atmos. Ocean. Technol., 14, 512–526, https://doi.org/10.1175/1520-0426(1997)014<0512:QCAFSP>2.0.CO;2, 1997.

Wang, Y., Chen, C., Mamtimin, A., Zhang, G., Gong, Q., Sayit, H., Peng, J., Gao, J., and Song, M.: Evolution Patterns of Carbon Flux in the Alpine Meadow Ecosystem, J. Geophys. Res. G: Biogeosciences., 130, https://doi.org/10.1029/2025JG009295, 2025.

Wang, Y., Xiao, J., Ma, Y., Ding, J., Chen, X., Ding, Z., and Luo, Y.: Persistent and enhanced carbon sequestration capacity of alpine grasslands on Earth's Third Pole, Sci. Adv., 9, eade6875, https://doi.org/10.1126/sciadv.ade6875, 2023.

Warren, C. R., and Taranto, M. T.: Ecosystem Respiration in a Seasonally Snow-Covered Subalpine Grassland, Arct. Antarct. Alp. Res., 43, 137–146, https://doi.org/10.1657/1938-4246-43.1.137, 2011.

White, M. D., and McMahon, A. R. G.: Vegetation assessment of the Perisher Range resort area: Report prepared for NSW National Parks and Wildlife Service, Ecology Australia Pty Ltd., Fairfield, Victoria, 2000.

Wood, S. N.: Fast stable restricted maximum likelihood and marginal likelihood estimation of semiparametric generalized linear models, J. R. Stat. Soc., B: Stat. Methodol., 73, 3–36, https://doi.org/10.1111/j.1467-9868.2010.00749.x, 2011.

Wood, S. N.: Generalized additive models : an introduction with R, 2nd edition, CRC Press, Taylor and Francis Group, https://doi.org/10.1201/9781315370279, 2017.

Worboys, G. L., and Good R. B.: Caring for our Australian Alps catchments: summary report for policy makers, Department of Climate Change and Energy Efficiency, Canberra, Australia, https://theaustralianalps.files.wordpress.com/2014/01/catchmentrpt2011_summary.pdf: last access: 5 May 2020, 2011.

Wutzler, T., Lucas-Moffat, A., Migliavacca, M., Knauer, J., Sickel, K., Šigut, L., Menzer, O., and Reichstein, M.: Basic and extensible post-processing of eddy covariance flux data with REddyProc, Biogeosciences, 15, 5015–5030, https://doi.org/10.5194/bg-15-5015-2018, 2018.

Wutzler, T., Reichstein, M., Moffat, A. M., and Migliavacca, M.: REddyProc: Post Processing of (Half) Hourly Eddy-Covariance Measurements, R package version 1.3.3, CRAN, https://CRAN.R-project.org/package=REddyProc, 2024.

Zhang, T.: Influence of the seasonal snow cover on the ground thermal regime: An overview, Rev. Geophys., 43, https://doi.org/10.1029/2004RG000157, 2005.

Zhao, L., Li, J., Xu, S., Zhou, H., Li, Y., Gu, S., and Zhao, X.: Seasonal variations in carbon dioxide exchange in an alpine wetland meadow on the Qinghai-Tibetan Plateau, Biogeosciences, 7, 1207–1221, https://doi.org/10.5194/bg-7-1207-2010, 2010.